Published online 16 April 2007

Nucleic Acids Research, 2007, Vol. 35, No. 9 ***2885–2892***
doi:10.1093/nar/gkm024

Specificity, duplex degradation and subcellular localization of antagomirs

Jan Krützfeldt[1,†], Satoru Kuwajima[1], Ravi Braich[2], Kallanthottathil G. Rajeev[2], John Pena[3], Thomas Tuschl[3], Muthiah Manoharan[2] and Markus Stoffel[1,†,*]

[1]Laboratory of Metabolic Diseases, The Rockefeller University, 1230 York Avenue, New York, NY 10021, USA, [2]Alnylam Pharmaceuticals Inc., 300 3rd Street, Cambridge, MA 02142 USA and [3]Howard Hughes Medical Institute, Laboratory of RNA Molecular Biology, The Rockefeller University, 1230 York Avenue, New York, NY 10021, USA

Received November 6, 2006; Revised and Accepted January 3, 2007

ABSTRACT

MicroRNAs (miRNAs) are an abundant class of 20–23-nt long regulators of gene expression. The study of miRNA function in mice and potential therapeutic approaches largely depend on modified oligonucleotides. We recently demonstrated silencing miRNA function in mice using chemically modified and cholesterol-conjugated RNAs termed 'antagomirs'. Here, we further characterize the properties and function of antagomirs in mice. We demonstrate that antagomirs harbor optimized phosphorothioate modifications, require >19-nt length for highest efficiency and can discriminate between single nucleotide mismatches of the targeted miRNA. Degradation of different chemically protected miRNA/antagomir duplexes in mouse livers and localization of antagomirs in a cytosolic compartment that is distinct from processing (P)-bodies indicates a degradation mechanism independent of the RNA interference (RNAi) pathway. Finally, we show that antagomirs, although incapable of silencing miRNAs in the central nervous system (CNS) when injected systemically, efficiently target miRNAs when injected locally into the mouse cortex. Our data further validate the effectiveness of antagomirs *in vivo* and should facilitate future studies to silence miRNAs for functional analysis and in clinically relevant settings.

INTRODUCTION

MiRNAs are an abundant class of non-coding RNA ranging from 20 to 23 nt of length that are post-transcriptional regulators of gene expression. MiRNAs have been mainly associated with developmental processes in metazoa such as *Caenorhabditis elegans* or *Drosophila melanogaster* (1). However, evidence also suggests a role for miRNAs in a wide range of functions in mammals, including insulin secretion, heart, skeletal muscle and brain development (2,3). Furthermore, miRNAs have been implicated in diseases such as cancer (4) and hepatitis C (5), which make them attractive new drug targets. In contrast to the widely used RNAi technology using small interfering RNA (siRNA) duplexes, strategies to inhibit miRNAs have been less well investigated. Reverse-complement 2′-*O*-methyl sugar modified RNA is frequently being used to block miRNA function in cell-based systems (6). The use of miRNA inhibitors in mice, however, remains challenging. Recently, two independent approaches to silence miRNAs *in vivo* have been reported. Our group demonstrated silencing of miRNAs in mice based on RNA analogs termed 'antagomirs' (7). Antagomirs are RNA-like oligonucleotides that harbor various modifications for RNAse protection and pharmacologic properties such as enhanced tissue and cellular uptake. They differ from normal RNA by complete 2′-*O*-methylation of sugar, phosphorothioate backbone and a cholesterol-moiety at 3′-end. Antagomirs efficiently silence miRNAs in most tissues after three injections at 80 mg/kg bodyweight (bw) on consecutive days. Esau *et al.* recently demonstrated a different strategy to silence miRNA(miR)-122 in mouse liver (8). They inhibited miR-122 following a four-week treatment protocol with two injections per week of 12.5–75 mg/kg bw of an antisense oligonucleotide (ASO) harboring a complete 2′-*O*-methoxyethyl and phosphorothioate modification.

Ultimately the efficient use of oligonucleotides to target miRNAs for functional studies and therapeutic use will be dependent on characterizations based on

*To whom correspondence should be addressed. Tel: +41 44 633 4560; Fax: +41 44 633 1051; E-mail: stoffel@imsb.biol.ethz.ch
†Present Address:
Institute for Molecular Systems Biology, Laboratory of Metabolic Diseases, ETH Zürich, Wolfgang Pauli Strasse 16, CH-8093 Zürich, Switzerland.

Table 1. Antagomirs of mir-122 and mir-16*

S. No	Sequence	Description
1	5′-UGGAGUGUGACAAUGGUGUUUGU-3′	Mir-122
2	5′-$a_s c_s$aaacaccauugucacacu$_s c_s c_s a_s$-Chol-3′	Antagomir-122 (23 nt, 6 × P=S)
3	5′-$c_s a_s$caaacaccauugucacacuc$_s c_s a_s c_s$-Chol-3′	Antagomir-122 (25 nt, 6 × P=S)
4	5′-$c_s a_s$aacaccauugucacac$_s u_s c_s c_s$-Chol-3′	Antagomir-122 (21 nt, 6 × P=S)
5	5′-$a_s a_s$acaccauugucaca$_s c_s u_s c_s$-Chol-3′	Antagomir-122 (19 nt, 6 × P=S)
6	5′-$a_s a_s$caccauugucac$_s a_s c_s u_s$-Chol-3′	Antagomir-122 (17 nt, 6 × P=S)
7	5′-acaaacaccauugucacacucca-Chol-3′	Antagomir-122 (23 nt, no P=S)
8	5′-acaaacaccauugucacacucca$_s$-Chol-3′	Antagomir-122, (23 nt, 1 × P=S)
9	5′-$a_s c_s a_s a_s c_s a_s c_s c_s a_s u_s u_s g_s u_s c_s a_s c_s a_s c_s u_s c_s c_s a_s$-Chol-3′	Antagomir-122, (23 nt, 23 × P=S)
10	5′-$a_s c_s$acacaacacugucacauu$_s c_s c_s a_s$-Chol-3′	mm-antagomir-122 (23 nt, 6 × P=S, 4 mm)
11	5′-$a_s c_s$aaacaccacugucacauu$_s c_s c_s a_s$-Chol-3′	mm-antagomir-122 (23 nt, 6 × P=S, 2 mm)
12	5′-$a_s c_s$aaacaccauugucacauu$_s c_s c_s a_s$-Chol-3′	mm-antagomir-122 (23 nt, 6 × P=S, 1 mm at nt19)
13	5′-$c_s c_s$aaacaccauugucacacu$_s c_s c_s a_s$-Chol-3′	mm-antagomir-122 (23 nt, 6 × P=S, 1 mm at nt1)
14	5′-$a_s c_s$aaacaccacugucacacu$_s c_s c_s a_s$-Chol-3′	mm-antagomir-122 (23 nt, 6 × P=S, 1 mm at nt11)
15	5′-UGGAGUGUGACAauGGUGUUUGU-3′	MiR-122 (2′-*O*-Me at 10 and 11)
16	5′-$U_s G_s$GAGUGUGACAAUGGUGUUU$_s G_s$U-3′	MiR-122 (2 × P=S at each end)
17	5′-Q570$_s$-$a_s$caaacaccauugucacacu$_s c_s c_s a_s$-Chol-3′	Antagomir-122 (5′-Quasar570)
18	5′-Q570$_s$-$a_s$cacacaacacugucacauu$_s c_s c_s a_s$-Chol-3′	Mm-antagomir-122 (4 mm, 5′-Quasar570)
19	5′-$c_s g_s$ccaauauuuacgugcug$_s c_s u_s a_s$-Chol-3′	Antagomir-16

*Lower case letters indicate 2′-*O*-methyl-modified nucleotides; subscript 's' indicates a phosphorothioate linkage and 'chol' represents cholesterol linked through a hydroxyprolinol linkage.

miRNA targets *in vivo*. Moreover, more efficient strategies could be developed through a more detailed understanding of the mechanisms of miRNA silencing. In this study, we begin to address these questions using regulation of endogenous miR-122 targets and fluorophore-tagged antagomirs.

MATERIALS AND METHODS

Synthesis of antagomirs

The single-stranded RNAs and modified RNA analogs (antagomirs) were synthesized as previously described (7). The oligonucleotides used in this study are listed in Table 1 and a schematic representation of the chemical modifications is shown in Figure 1. Quasar-570 (Q570) phosphoramidite from Biosearch Technologies was coupled to the 5′-terminal under standard solid-phase phosphoramidite synthesis conditions to obtain fluorophore-tagged antagomir 122 and mm-antagomir-122. Extended 15-min coupling of quasar-570 phosphoramidite was carried out at a concentration of 0.1 M in CH_3CN in the presence of 5-(ethylthio)-1*H*-tetrazole activator followed by standard capping, oxidation and deprotection afforded labeled oligonucleotides. The Q570 conjugated sequences were HPLC purified on an in-house packed RPC-Source15 reverse-phase column. The buffers were 20 mM NaOAc in 10% CH_3CN (buffer A) and 20 mM NaOAc in 70% CH_3CN (buffer B). Fractions containing full-length oligonucleotides were pooled and desalted. Analytical HPLC, CGE and ES LC-MS established the integrity of the compounds. For duplex generation, equimolar amounts of miR-122 and antagomir were heated in 1 × PBS at 95°C for 5 min and slowly cooled to room temperature.

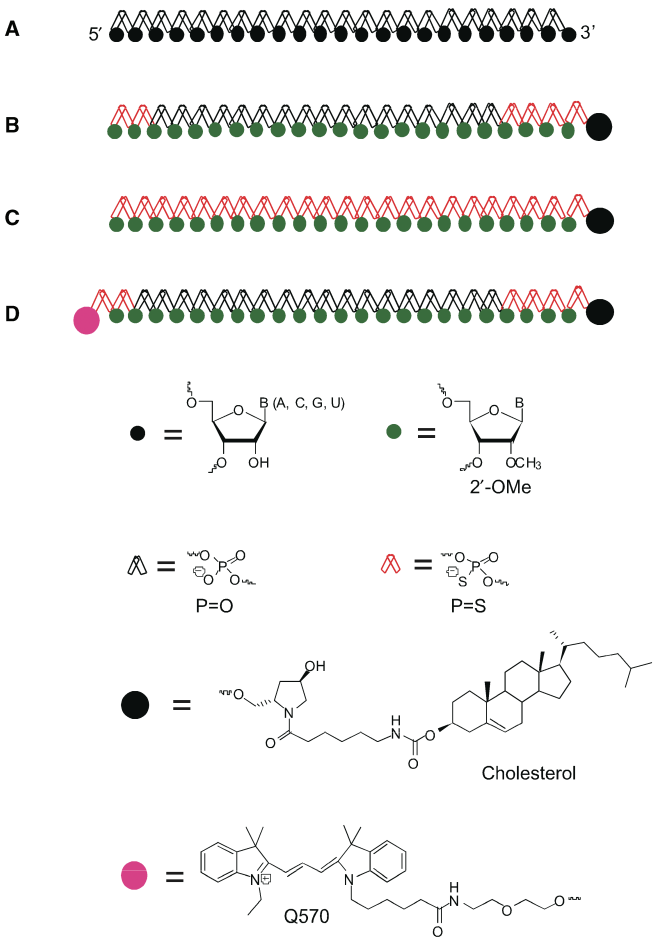

Figure 1. Chemical modifications used in this study. Schematic representation of (**A**) miR-122, (**B**) antagomir-122, (**C**) antagomir-122 all P=S and (**D**) 5′-Quasar570 labeled antagomir-122.

Animals

All animals were maintained in a C57Bl/6J background on a 12-h light–dark cycle in a pathogen-free animal facility at Rockefeller University. Six-week-old mice received on three consecutive days tail vein injections of saline or different RNAs in 0.2 ml per injection at normal pressure. Liver tissue was harvested 24 h after the last injection or as otherwise indicated.

For cerebral injections, mice were anaesthetized and antagomir-16 was injected into the left frontal cortex (~800 ng). Injections of equal volume PBS into the contralateral area of the right hemisphere served as controls. After 72 h mice were sacrificed, blood was removed through systemic perfusion of the left ventricle with PBS and a ~0.4 cm^3 area surrounding the injection site excised from the cortex.

Northern blotting analysis

Total RNA was isolated using the Trizol protocol with ethanol precipitation and northern blot analysis was performed using formamide-containing PAGE as previously described (7).

RT-PCR

Extraction of total RNA, synthesis of cDNA, and PCR were performed as previously described (7). Primer sequences and annealing temperatures are shown in supplementary materials.

Sucrose density gradient fractionation of liver homogenates

Mice were perfused with ice-cold PBS through the left ventricle and ~100 mg liver tissue excised. Cells were fractionated on continuous sucrose density gradients from 0.4 to 2 M as described earlier (9). Fractions were separated on 14% PAGE containing 8 M urea and 20% formamide. Concentration of 5′-Q570-labeled antagomir in liver fractions was measured using an fmax spectrophotometer from Molecular devices.

Immunofluorescence

For immunofluorescence of P-bodies and antagomirs, 1 mg of Q570-labeled antagomirs were injected in 0.2 ml and normal pressure on Day 1, followed by injection of 50 μg of a Gfp-GW182-expressing DNA-plasmid (10; kindly provided by Dr E.K. Chan, Gainesville, Florida, USA) in 2 ml PBS and high pressure on Day 2. On Day 3 mice were anesthetized and perfused through the left ventricle with 2% paraformaldehyde. Livers were incubated overnight at 4°C in 4% paraformaldehyde, followed by 16-h incubation in 30% sucrose/PBS (v/v). Frozen sections (7 μm) were mounted on glass slides and analyzed using a laser-scanning microscope.

Statistical analysis

Results are given as means. Statistical analysis was performed with Student's *t*-test, and the null hypothesis was rejected at the 0.05 level.

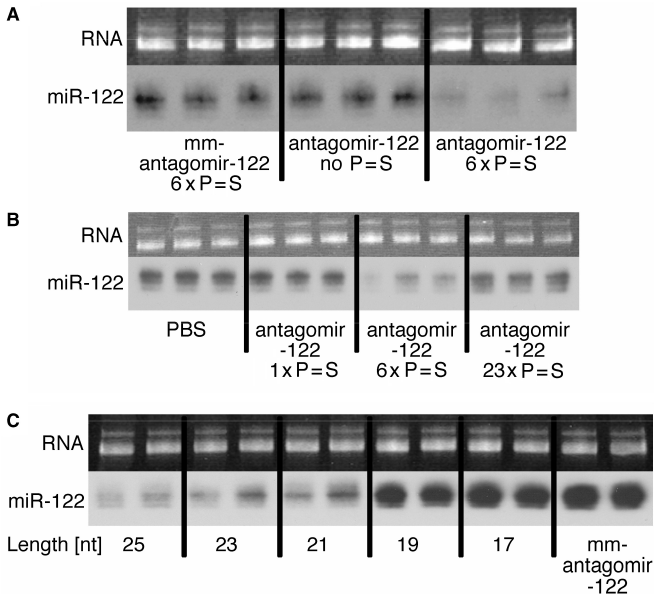

Figure 2. Impact of antagomir phosphorothioate modifications and antagomir length on miR-122 levels. Northern blots of total RNA isolated from livers of mice that were treated with different antagomir-122 chemistries at 3 × 20 mg/kg bw. (**A,B**) Different phosphorothioate modifications; (**C**) different lengths. 'P=S' indicates phosphorothioate modification. Each lane represents an individual animal.

RESULTS

Phosphorothioate modifications and length of antagomir-122

The antagomir-122 chemistry includes six phosphorothioate backbone modifications. Two phosphorothioates are located at the 5′-end and four at the 3′-end. To test whether the number of phosphorothioates is critical for the ability of antagomir-122 to silence miR-122, we compared four different antagomir-122 molecules that only differ in the number of phosphorothioate modification (P=S). Injection of antagomir-122 at 3 × 20 mg/kg bw with no P=S into mice did not influence miR-122 levels in the liver (Figure 2A). The addition of a single P=S did not alter miR-122 levels either as compared to the antagomir-122 with six P=S (Figure 2B). Intriguingly, complete P=S modification of the antagomir-122 did not further increase the effect on miR-122 levels (Figure 2B). These results demonstrate that phosphorothioates are important for antagomir-122 function, however, complete replacement of P=O by P=S decreases its efficiency. The result can be explained by the enhanced stability provided by the terminal P=S-linked antagomir and the reduced thermodynamic stability of the fully modified P=S antagomir duplex with targeted miRNA.

We also determined the optimal nucleotide length of antagomirs for silencing endogenous miR-122 levels *in vivo*. Addition of two nucleotides or shortening of antagomir-122 by two nucleotides did not significantly alter its efficiency (Figure 2C). However, silencing of miR-122 was abolished at 3 × 20 mg/kg bw when the length of antagomir-122 was reduced to 19 nt. Together, these results further elicit the requirement of optimum number of phosphorothioate modifications and minimum

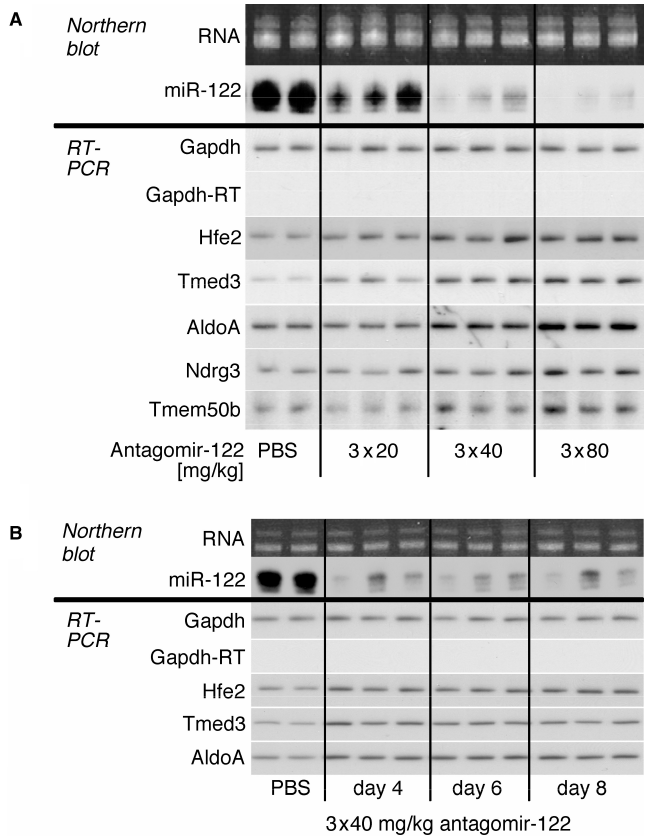

Figure 3. Dose- and time-dependency of miR-122 target regulation by antagomir-122. Steady-state mRNA levels of miR-122 target genes in livers of mice treated with the indicated amounts of antagomir-122. Expression was measured by RT-PCR. Each lane indicates an individual animal. The glyceraldehyde-3-phosphate dehydrogenase gene (Gapdh) was used as a loading control. Gapdh-RT denotes a control without reverse transcription. Gene symbols are shown in accordance with the International Standardized Nomenclature (www.informatics.jax.org/mgihome/nomen/gene.shtml). The upper row shows a northern blot of liver RNA for miR-122. Each lane represents an individual animal. (**A**) Dose-dependency. (**B**) Time-course.

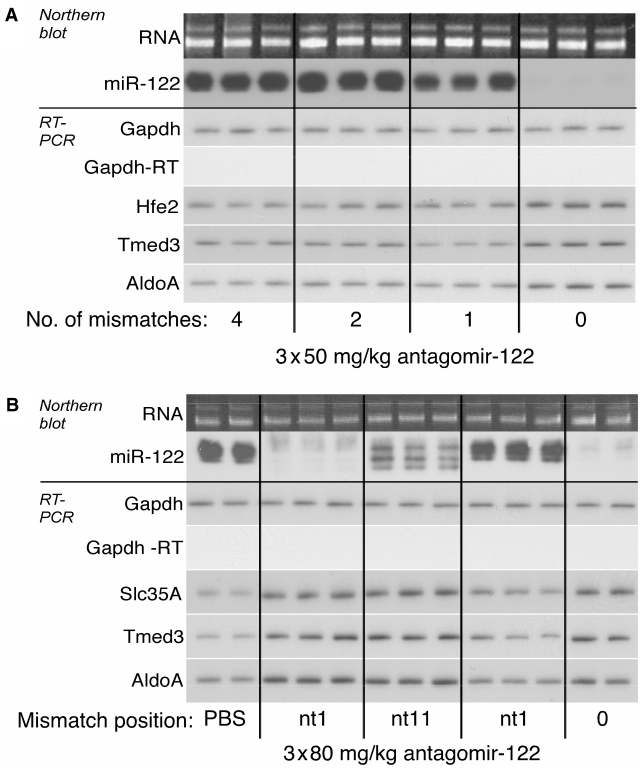

Figure 4. Sequence discrimination of antagomir-*122*. Steady-state mRNA levels of miR-122 target genes in livers of mice treated with the indicated amounts of antagomir-122 or antagomir-122 that harbored 4, 2 or 1 nt mismatches, respectively (**A**), or 1-nt mismatch at different positions (**B**). Expression was measured using RT-PCR. Gapdh was used as a loading control, Gapdh-RT denotes a control without reverse transcription. Each lane represents an individual animal.

length of antagomirs for their biological function *in vivo*. The tendency for improved activity of 25-mer antagomir can be explained on the basis of improved thermodynamic binding affinity of the 25 mer, which should also have higher biostability from exonucleases for the core 23 mer.

Dose- and time-dependency of antagomir-122

To investigate the optimal dose- and time-dependency of antagomir-122, we analyzed miR-122 levels as well as mRNA levels of endogenous miR-122 targets. Northern blots show that optimal reduction of miR-122 levels is achieved at antagomir concentrations between 3×40 and 3×80 mg/kg bw (Figure 3A). The effect of 3×40 mg/kg on miR-122 levels is stable for at least 8 days (=5 days after the last injection) (Figure 3B). The expression of miR-122 targets correlated with the reduction of miR-122 levels in northern blots and showed highest upregulation at antagomir concentrations between 3×40 and 3×80 mg/kg bw (Figure 3A). All targets analyzed showed stable upregulation for at least 5 days after the last injection (Figure 3B). Together, the results demonstrate that robust and lasting upregulation of miR-122 targets is achieved at antagomir concentrations between 3×40 and 3×80 mg/kg bw as early as 24 h after the last injection.

Mismatch discrimination of antagomirs

We tested the impact of different mismatch numbers in the antagomir sequence on miR-122 levels and miR-122 targets. Four mismatches, two mismatches or a single mismatch at position 19 was sufficient to prevent downregulation of miR-122 and upregulation of three different miR-122 targets (AldoA, Tmed3 and Hfe2) as measured by RT-PCR (Figure 4A). However, single nucleotide mismatches at two different positions (nt1 or nt11) did not prevent downregulation of miR-122 levels or target regulation (Figure 4B). These data demonstrate that antagomirs can exhibit high sequence specificity. However, discrimination at the single nucleotide level is position-dependent and has to be tested for each microRNA sequence that is being targeted.

Regulation of miR-122 targets by stabilized duplexes of miR-122/antagomir-122

We asked whether antagomir-mediated miRNA silencing involves degradation of the miRNA by analyzing the

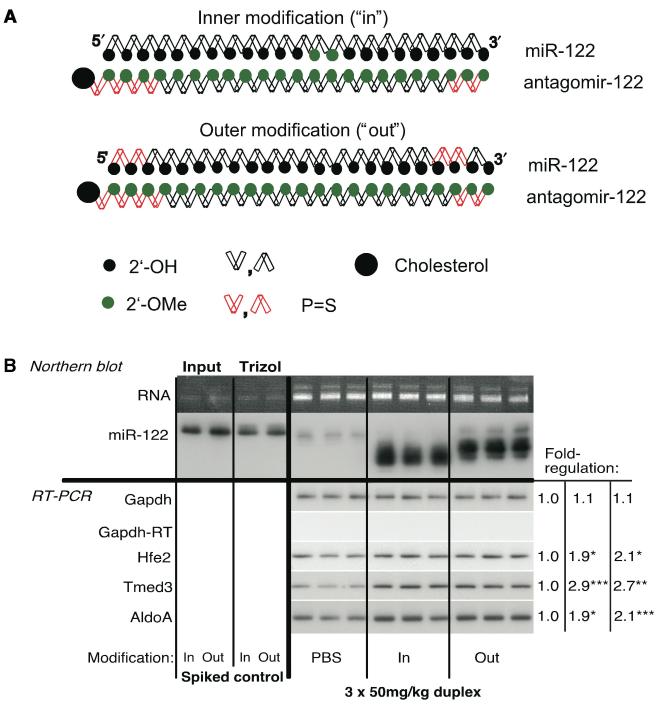

Figure 5. Regulation of miR-122 targets by chemically protected antagomir-122/miR-122-duplexes. (**A**) Schematic description of the two different duplexes used. (**B**) Steady-state mRNA levels of miR-122 target genes in livers of mice treated with the indicated modified antagomir-122/miR-122-duplexes. Expression was measured using RT-PCR. Fold-regulation indicates the ratio of expression levels of the means of mice treated with antagomir-122/miR-122 duplex compared to the PBS group. The upper row shows a northern blot of liver RNA for miR-122. As controls, duplexes were added to 5 µg total kidney RNA and loaded on polyacrylamide gels before ('input') or after the Trizol protocol ('Trizol'). Each lane represents an individual animal. Gapdh was used as a loading control, Gapdh-RT denotes a control without reverse transcription. $^{*}P<0.05$; $^{**}P<0.01$; $^{***}P<0.001$; Student's *t*-test compared to PBS.

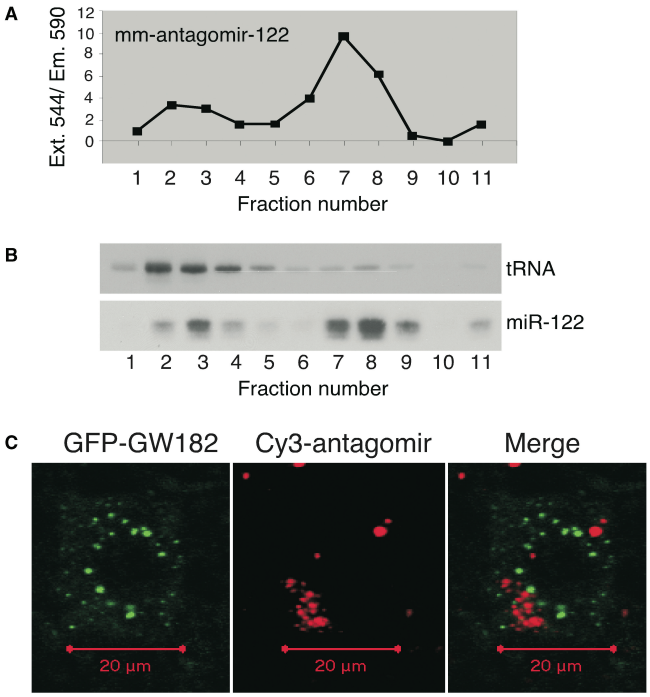

Figure 6. Localization of antagomir-122 and miR-122 in hepatocytes. Liver tissue from mice that were treated with 3×80 mg/kg Q570-labeled mm-antagomir-122 was fractionated on a sucrose gradient following ultracentrifugation. Localization of Q570-labeled mm-antagomir-122 was analyzed by spectrophotometry (**A**), localization of t-RNA and miR-122 were analyzed using northern blotting of total RNA isolated from each fraction (**B**). For subcellular localization of antagomirs and P-bodies in mouse liver, mice were treated with Q570-labeled antagomir-122 and a DNA-plasmid expressing a GFP-GW182 hybrid as described in the Materials and Methods section. P-body and Q570-antagomir localizations were visualized using laser-scanning microscopy (**C**).

ability of antagomirs to induce degradation of preformed duplexes. We synthesized duplexes of antagomir-122 and a synthetic miR-122 that harbored modifications to protect against different RNAse activities. MiR-122 was either protected at the outside ('out') with a phosphorothioate modification to protect against exonucleases or at two consecutive internal positions (nt13 and nt14 of miR-122; 'in') using 2′-*O*-methyl sugar modification (Figure 5A) to protect against endonuclease activity. Injection of both types of duplexes led to the appearance of degradation products of the synthetic miR-122 (Figure 5B). These degradation products did not appear when the duplexes were directly analyzed on the polyacrylamide gels or after they had been subjected to the RNA isolation protocol (Figure 5B, 'spiked control'). Furthermore, the spiked control data demonstrate that the synthetic miRNA was not lost during the isolation procedure. These data show that both types of stabilized miR-122 that were bound to the antagomir-122 had been degraded. Accordingly, both types of protected duplexes upregulated three different miR-122 targets (Figure 5B). We conclude that antagomir-mediated-silencing of miRNAs involves target degradation. However, this process does not depend on exonuclease activity and seems to differ from the RNAi pathway.

Cellular localization of antagomirs

To localize antagomirs and miRNA in subcellular compartments, we used 5′-Q570-labeled antagomir-122 or Q570-labeled mm-antagomir-122. Q570-labeling did not impair antagomir-122 function, although silencing efficiency was slightly decreased (data not shown). First, we fractionated liver homogenates from mice that had been treated with Q570-mm-antagomir-122 by ultracentrifugation on sucrose gradients. Northern blot analysis of various fractions showed a single peak of tRNA in fraction 2 (Figure 6A). In contrast, miR-122 and mm-antagomir-122 localized both to two peaks, fraction 2/3 and fraction 7/8 (Figure 6B). We next investigated whether co-localization of antagomirs and miRNAs involves the P-body compartment. To visualize P-bodies in mouse liver *in vivo* we used a GFP-expressing construct (GFP-GW182) that has previously been demonstrated to act as a marker for the P-body compartment (10). We overexpressed GFP-GW182 in liver using high-pressure high-volume tail vein injections and analyzed GFP- and Q570-fluorescence with laser-scanning microscopy.

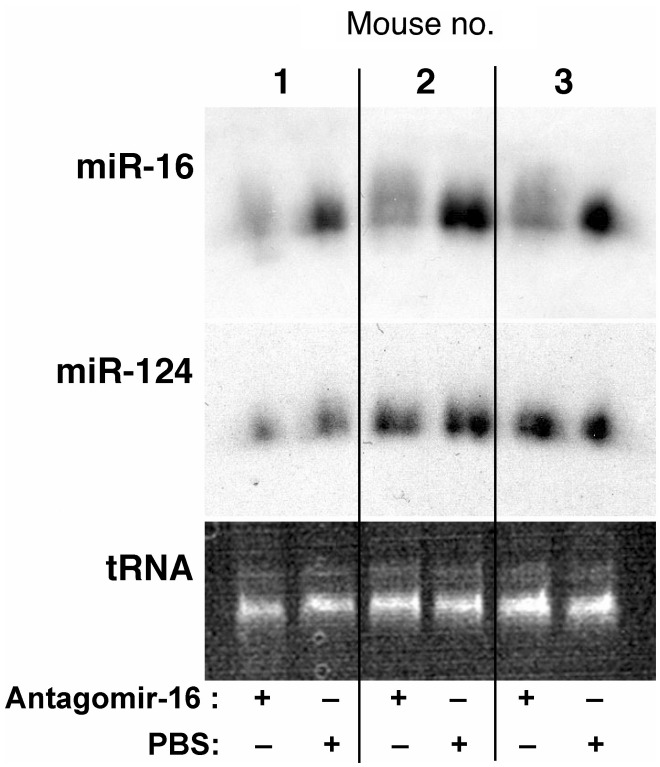

Figure 7. Injection of antagomir-16 into mouse cortex. Northern blots of miR-16 and miR-124 from total RNA isolated from mouse cerebral cortex that had been injected with antagomir-16 or PBS into the right and left cerebral hemispheres, respectively. Each pair of lanes represents an individual animal.

Q570-labeled antagomirs were exclusively localized in the cytosol and distinct from P-bodies (Figure 6C). There was no overlap between these two compartments. Together, we conclude that antagomirs and miRNA interact in a cytoplasmic compartment upstream of P-bodies.

Intracerebral application of antagomirs

We previously described that systemic injections of antagomir-16 into tail veins of mice do not influence the steady-state levels of miR-16 in the brain. MiR-16 is ubiquitously expressed including neurons. We tested whether antagomir-16 can decrease miRNA levels in the brain when injected directly into the cortex of anesthetized mice. PBS injections into the contra lateral side of the same animal served as controls. A single injection of ~0.8 μg of antagomir led to a robust decrease in miR-16 expression at 3 days after the injection (Figure 7). These results demonstrate that direct application of antagomirs can efficiently target miRNAs in tissues that cannot be reached through tail vein injections.

DISCUSSION

In this study, we characterized the inhibition of miRNAs with antagomirs *in vivo*. A detailed understanding of this process is needed to investigate miRNA function in mice and exploit their therapeutic potential. Our study provides a unique platform since its major read-out is based on the dose-and time-dependent regulation of several endogenous and validated targets of miR-122.

Specificity of drug-like oligonucleotides is important to minimize off-target effects and to discriminate between related miRNAs that sometimes differ by only a single nucleotide. Previous studies have demonstrated that locked nucleic acid (LNA) are sensitive to single mismatch in *in-situ* staining protocols of zebrafish embryos (11). Tissue-culture-based luciferase assays indicated that 2′-*O*-methoxyethyl oligonucleotides might have a similar specificity (12). In line with these data we show that the antagomir chemistry enables discrimination of a single nucleotide. Intriguingly, this effect depends on the position of the mismatch within the antagomir sequence. Nucleotide exchanges at the very 5′-end of the antagomir or in the center did not prevent downregulation of miR-122 levels in northern blots and upregulation of miR-122 targets. This observation is in agreement with the work published by Davis *et al.*, who reported a similar result in luciferase-based assays (12). Asymmetry of a single nucleotide mismatch may therefore be more detrimental for targeting miRNAs than symmetric changes. These data are important for the design of antagomirs that target specific members of miRNA families or when off-target effects have to be considered.

The mechanism of oligonucleotide-mediated miRNA silencing is still unknown. Previous data from our group and others suggested that this process involves degradation of the miRNA *in vitro* (12) and *in vivo* (7,8). Northern blots of tissue samples treated with antagomirs fail to detect fragments of the targeted miRNA. This could be explained by cellular RNase activity that readily degrades them. We have previously demonstrated that increasing the cellular amount of endogenous miRNA by introducing duplexes of miRNA/antagomir leads to detectable degradation products (7). In this study, we used this approach to ask whether antagomir-mediated silencing of miRNA involves a RNA-induced silencing complex (RISC)-dependent cleavage mechanism. In the RNAi pathway, the siRNA duplex of passenger strand and guide strand is integrated into the RISC complex and the argonaute-2 (Ago2) protein subsequently cleaves the passenger strand across from the guide strand's phosphate bond between position 10 and 11 (13,14). This cleavage was inhibited by a single 2′-*O*-methylation of the passenger strand corresponding to nucleotide 11 of the guide strand (13). Hypothetically, antagomirs could cleave miRNAs within RISC with the antagomir acting as the guide strand. To test this, we injected miRNA/antagomir-duplexes into mice that harbored a 2′-*O*-methyl endonuclease protection of the microRNA corresponding to nucleotide 10 and 11 of the antagomir. However, endonuclease protection between nucleotides 10 and 11 did not prevent the degradation of the miRNA as demonstrated by abundant miRNA fragments in northern analysis, nor did it prevent the upregulation of miR-122 targets. Thus Ago2-mediated cleavage is unlikely to mediate this process. Similar results were obtained when the miRNA was protected at the outside positions using

phosphorothioates, indicating that the miRNA targeting does not dependent on exonuclease activity either. However, the fact that miRNA/antagomir-duplexes regulate miRNA targets suggests antagomir recycling. The appearance of miRNA fragments of decreased length suggests that degradation is involved in this recycling process. Further elucidation of the mechanism of degradation will be important for optimizing miRNA silencing.

To address the subcellular compartment where interaction of miRNA and antagomir occurs we engineered flurophore-labeled antagomirs. Flurophore labeling of siRNA has previously been used to evaluate cellular uptake of siRNA (15,16). Q570-labeled antagomirs were cleared from the plasma at a $t_{1/2}$ of ~30 min (data not shown), which is considerably faster than the plasma-clearance of cholesterol-conjugated siRNA of ~90 min (17). A striking overlap of the subcellular localization profiles of antagomirs and miRNAs by sucrose gradient ultracentrifugation analysis of liver homogenates indicates that they might share subcellular compartments. Antagomir localization within hepatocytes was strictly limited to the cytosol. This could explain why antagomirs did not influence steady-state levels of the nuclear precursors of miRNAs (7). We asked whether antagomirs could localize to P-bodies, since this compartment has been linked to the miRNA pathway. P-bodies are enriched in Ago 2 as well as mRNA that is targeted by miRNAs. It is, however, still unknown to which degree endogenous miRNAs localize to P-bodies. In any case, we did not observe any co-localization of antagomirs and P-bodies and conclude that the interaction of antagomirs and miRNAs occurs upstream of this compartment.

In this study, we also extended our previous analysis of the influence of different chemical modifications on antagomirs. Phosphorothioate modifications provide protection against RNase activity and their lipophilicity contributes to enhanced tissue uptake. On the other hand, phosphorothioates decrease the melting temperature of RNA duplexes (12) and have been shown to be general inhibitors of cellular RNAse activity (18). Indeed our results indicate a critical balance of the number of phosphorothioates within the antagomir chemistry. While a significant number of phosphorothioates increases efficiency, complete phosphorothioate modification decreased efficiency. Our data also demonstrate that antagomirs require >19-nt length for optimal function.

Lastly, we demonstrate that antagomirs can efficiently decrease miR-16 levels in mouse brain when injected locally. Systemic infusions of antagomir-16 do not change brain levels of miR-16, most likely because of an inability to cross the blood-brain barrier (7). Local injections of small amounts of antagomir-16 efficiently reduced expression of this miR-16 in the cortex. This inhibition was specific since the expression of other miRNAs was not affected and no alteration in miR-16 levels were measured in the contralateral hemisphere that was injected with PBS. These results suggest that miRNA-inhibitors could facilitate the elucidation of miRNA function in the CNS.

Different chemical modifications have been described to block miRNA function *in vitro* (6,12) or *in vivo* (7,8). However, detailed characterizations of these inhibitors are either lacking or based on heterologous miRNA target reporter assays (12). In this study, we used the expression levels of endogenous miR-122 targets as a read-out. We show that antagomirs can be used in a time- and dose-dependent fashion to study miRNA targets. Furthermore, we characterized antagomirs with regard to specificity, functional minimal-length requirements and effectiveness in the CNS following direct application. Our data support the conclusion that antagomirs will be powerful tools for further studies on miRNA function in mice and possibly non-rodent models and enhance the validation of miRNA inhibitors as potential therapeutics.

ACKNOWLEDGEMENT

This work was supported by the National Institutes of Health (grant 1 P01 GM073047) and the Howard Hughes Medical Institute. Funding to pay the Open Access publication charge was provided by the Swiss Federal Institute of Technology.

Conflict of interest statement. M.S. and T.T. are SAB members of Aluylam Pharmaceuticals, T.T. is a co-founder.

REFERENCES

1. Ambros,V. (2004) The functions of animal microRNAs. *Nature*, **431**, 350–355.
2. Kloosterman,W.P. and Plasterk,R.H. (2006) The diverse functions of microRNAs in animal development and disease. *Dev. Cell*, **11**, 441–450.
3. Krutzfeldt,J. and Stoffel,M. (2006) MicroRNAs: a new class of regulatory genes affecting metabolism. *Cell Metab.*, **4**, 9–12.
4. Esquela-Kerscher,A. and Slack,F.J. (2006) Oncomirs – microRNAs with a role in cancer. *Nat. Rev. Cancer*, **6**, 259–269.
5. Jopling,C.L., Yi,M., Lancaster,A.M., Lemon,S.M. and Sarnow,P. (2005) Modulation of hepatitis C virus RNA abundance by a liver-specific MicroRNA. *Science*, **309**, 1577–1581.
6. Krutzfeldt,J., Poy,M.N. and Stoffel,M. (2006) Strategies to determine the biological function of microRNAs. *Nat. Genet.*, **38**, S14–S19.
7. Krutzfeldt,J., Rajewsky,N., Braich,R., Rajeev,K.G., Tuschl,T., Manoharan,M. and Stoffel,M. (2005) Silencing of microRNAs *in vivo* with 'antagomirs'. *Nature*, **438**, 685–689.
8. Esau,C., Davis,S., Murray,S.F., Yu,X.X., Pandey,S.K., Pear,M., Watts,L., Booten,S.L., Graham,M. *et al.* (2006) miR-122 regulation of lipid metabolism revealed by *in vivo* antisense targeting. *Cell Metab.*, **3**, 87–98.
9. Ort,T., Maksimova,E., Dirkx,R., Kachinsky,A.M., Berghs,S., Froehner,S.C. and Solimena,M. (2000) The receptor tyrosine phosphatase-like protein ICA512 binds the PDZ domains of beta2-syntrophin and nNOS in pancreatic beta-cells. *Eur. J. Cell Biol.*, **79**, 621–630.
10. Eystathioy,T., Chan,E.K., Tenenbaum,S.A., Keene,J.D., Griffith,K. and Fritzler,M.J. (2002) A phosphorylated cytoplasmic autoantigen, GW182, associates with a unique population of human mRNAs within novel cytoplasmic speckles. *Mol. Biol. Cell*, **13**, 1338–1351.
11. Kloosterman,W.P., Wienholds,E., de Bruijn,E., Kauppinen,S. and Plasterk,R.H. (2006) In situ detection of miRNAs in animal embryos using LNA-modified oligonucleotide probes. *Nat. Methods*, **3**, 27–29.
12. Davis,S., Lollo,B., Freier,S. and Esau,C. (2006) Improved targeting of miRNA with antisense oligonucleotides. *Nucleic Acids Res.*, **34**, 2294–2304.
13. Rand,T.A., Petersen,S., Du,F. and Wang,X. (2005) Argonaute2 cleaves the anti-guide strand of siRNA during RISC activation. *Cell*, **123**, 621–629.

14. Matranga,C., Tomari,Y., Shin,C., Bartel,D.P. and Zamore,P.D. (2005) Passenger-strand cleavage facilitates assembly of siRNA into Ago2-containing RNAi enzyme complexes. *Cell*, **123**, 607–620.
15. Grunweller,A., Gillen,C., Erdmann,V.A. and Kurreck,J. (2003) Cellular uptake and localization of a Cy3-labeled siRNA specific for the serine/threonine kinase Pim-1. *Oligonucleotides*, **13**, 345–352.
16. Lingor,P., Koeberle,P., Kugler,S. and Bahr,M. (2005) Down-regulation of apoptosis mediators by RNAi inhibits axotomy-induced retinal ganglion cell death *in vivo*. *Brain*, **128**, 550–558.
17. Soutschek,J., Akinc,A., Bramlage,B., Charisse,K., Constien,R., Donoghue,M., Elbashir,S., Geick,A., Hadwiger,P. *et al*. (2004) Therapeutic silencing of an endogenous gene by systemic administration of modified siRNAs. *Nature*, **432**, 173–178.
18. Crooke,R.M., Graham,M.J., Martin,M.J., Lemonidis,K.M., Wyrzykiewiecz,T. and Cummins,L.L. (2000) Metabolism of antisense oligonucleotides in rat liver homogenates. *J. Pharmacol. Exp. Ther.*, **292**, 140–149.